

Original Research

Analysis of Mapping and Landscape Pattern Evolution in the Yellow River Delta Wetland in the Last 20 years

Zengliang Chang¹, Hongju Tong¹, Shouchao Hu¹, Can Zhang^{2*}

¹Shandong Electric Power Engineering Consulting Institute Corp., Ltd., Jinan, China

²School of Surveying and Geo-Informatics, Shandong Jianzhu University, Jinan, China

Received: 15 February 2024

Accepted: 13 April 2024

Abstract

Understanding the evolutionary process of land use and the landscape pattern of the Yellow River Delta wetland is an important prerequisite for promoting its sustainable development. In this study, we combined Landsat-5/7/8 data with the random forest algorithm to map the land cover/land use from 2002 to 2021 in the Yellow River Delta wetland and evaluated and analyzed them. The result demonstrated that: (1) the classification method used is promising, with an average OA and Kappa coefficient of 90.5% and 0.891, respectively; (2) the built-up area of Dongying District and some townships has been expanded since 2008; wheat fields are in Guangrao County, while paddy fields are in the northern part of Xicheng in Dongying District, in the east of the built-up area of Hekou District, and in the high-standard farmland project area; tamarisk shrubs are in the northeastern part, and suaeda meadows near the tidal flat; tidal flats, breeding aquatics, and saltern are in the eastern and northern parts; cropland accounted for the largest proportion, but smaller food cropland during 2002-2016; (3) the decreased woodland in the study area was converted to cropland, and the unused land was converted to waters, impervious surfaces, and cropland; (4) the landscape fragmentation, shape complexity, and aggregation were all reduced firstly and then increased with 2008 as the turning point. The research on mapping and landscape pattern evolution analysis in the Yellow River Delta wetland can provide references for environmental protection and urban and rural development.

Keywords: random forest, feature extraction, land use, landscape pattern, Yellow River Delta

Introduction

Land serves as the foundation of urban development [1]. With escalating urbanization and pervasive human activities, the land use and cover patterns within

the Yellow River Delta wetland region have undergone profound changes. Land use and cover changes (LUCC) wield significant influence over biodiversity and ecosystems [2-5]. In recent years, vast swaths of agricultural land in the Yellow River Delta wetland have been replaced by urban lands and industrial areas, disrupting the delicate balance of the ecosystem. Through the examination of land use changes

*e-mail:2023160105@stu.sdjzu.edu.cn

Tel.: +86-156-3386-7851

in the Yellow River Delta wetland, valuable insights emerge, offering crucial references and lessons for future resource management, environmental conservation, and urban-rural development endeavors.

Studies on wetland mapping in the Yellow River Delta region have predominantly relied on remote sensing techniques thus far. For instance, research investigating land use types and their dynamic changes in the region encompasses a range of aspects, including land cover types [6], wetland classification [7], information on saline and alkaline lands [8], spatial and temporal land use change patterns and drivers [9], as well as analysis of cropland degradation and its underlying causes [10]. These studies utilize various remote sensing techniques and methodologies, such as supervised classification [6], decision tree classification, visual interpretation [7], object-oriented classification, support vector machines [11], and tasseled cap transformation [12]. However, these studies exhibit certain limitations: some are confined to single counties or cities [8, 9, 11] and lack comprehensive coverage of the entire region; others focus solely on specific features like saline soils [8] or arable land [10] without conducting a comprehensive classification. Even when a comprehensive classification is undertaken, the division of land use types may be coarse, the study duration short, and the number of image periods insufficient [6] for long-term dynamic monitoring. Moreover, machine learning methods have been underutilized in these studies. V.F. Rodriguez-Galiano et al. demonstrated that the random forest algorithm can enhance the accuracy of land cover classification and outperform a single decision tree [13]. Therefore, adopting the random forest algorithm for mapping in the Yellow River Delta wetland is deemed feasible.

Based on the above discussion, this paper combines feature extraction with the employment of the random

forest algorithm to classify land use in the Yellow River Delta using five-phase Landsat-5/7/8 images from 2002 to 2021, evaluating the accuracy of the classification results. Finally, it conducts analyses on land use change and landscape pattern change with the aim of promoting sustainable development and ecological environmental protection in the Yellow River Delta region.

Material and Methods

Study Area and Data Sources

Study Area

The Yellow River Delta ($36^{\circ}55'N$ to $38^{\circ}10'N$, $118^{\circ}07'E$ to $119^{\circ}10'E$) predominantly encompasses Dongying, Kenli, Hekou, Lijin, and Guangrao counties in Shandong Province [14], as depicted in Fig. 1. Adjacent to the Bohai Sea, the Yellow River Delta boasts the most comprehensive wetland ecosystem within the Chinese warm temperate zone, thus exhibiting a diverse array of vegetation types [15]. Vegetation in the Yellow River Delta is categorized into artificial and natural vegetation. Artificial vegetation comprises crops and man-made forests. Crops such as wheat, corn, and rice are cultivated, while artificial forests primarily consist of acacia and dry willow trees. Crop cultivation follows a biennial cycle, employing crop rotation between wheat and corn [16]. Natural vegetation includes winged alkali flora, tamarisk scrub, reed scrub, and others [17]. The Yellow River Delta, characterized by its flat terrain and abundant mineral, hydrological, and land resources, offers ample space for development.

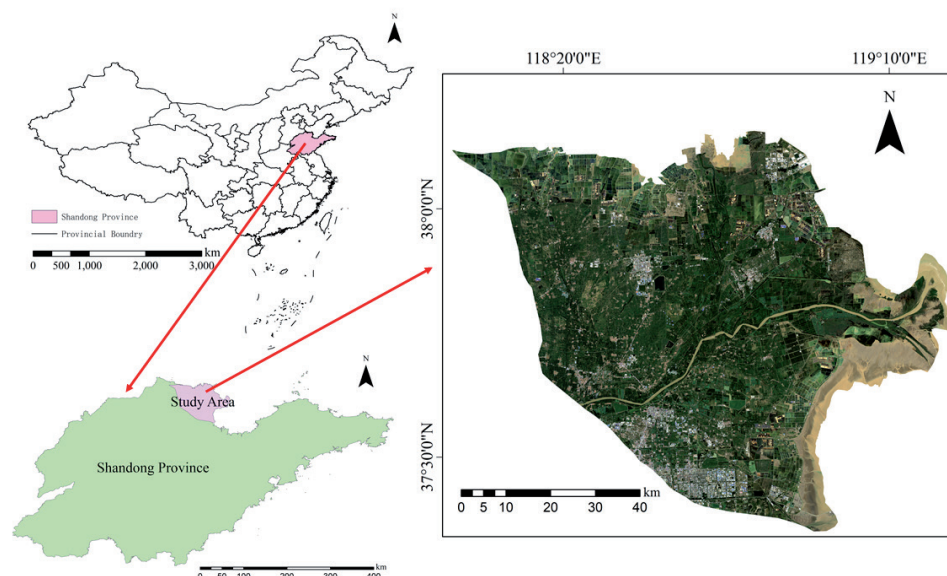


Fig. 1. Study area.

Data Source and Processing

The remote sensing data utilized in this study encompasses Landsat-5, Landsat-7, and Landsat-8, spanning the years 2002, 2008, 2016, 2018, and 2021, with a spatial resolution of 30 meters. For Landsat-5 TM and Landsat-7 ETM+ data, bands {1, 2, 3, 4, 5, 7} were selected. For Landsat-8 OLI data, bands {1, 2, 3, 4, 5, 6, 7} were utilized. The Landsat data employed are geometrically fine-corrected Level-1 Terrain (L1T) products, necessitating pre-processing steps such as radiometric calibration and atmospheric corrections before subsequent analysis.

Research Methods

The technical process of land use information extraction in this study is shown in Fig. 2, and the main steps are (1) image downloading and preprocessing; (2) feature extraction; (3) classification scheme development and sample selection; (4) random forest model training; (5) land use information extraction and accuracy evaluation.

Feature Extraction

The features utilized in this study encompass surface reflectance features, spectral index features (NDVI,

SAVI, and MNDWI), tasseled cap transform features (brightness, greenness, and humidity), and second-order texture features.

Spectral indices can be used to assist in distinguishing between different classes of features [18]. In this study, the spectral indices utilized include NDVI (Normalized Difference Vegetation Index) [19], SAVI (Soil Adjusted Vegetation Index) [18, 20], and MNDWI (Modified Normalized Difference Water Index) [21], applied as follows:

$$NDVI = \frac{\rho(NIR) - \rho(Red)}{\rho(NIR) + \rho(Red)} \tag{1}$$

$$SAVI = \frac{\rho(NIR) - \rho(Red)}{\rho(NIR) + \rho(Red) + L} \times (1 + L) \tag{2}$$

$$MNDWI = \frac{\rho(Green) - \rho(MIR)}{\rho(Green) + \rho(MIR)} \tag{3}$$

where $\rho(Green)$, $\rho(Red)$, $\rho(NIR)$, and $\rho(MIR)$ respectively represent the surface reflectance of the green, red, near-infrared, and mid-infrared, with L being an empirical value set to 0.5.

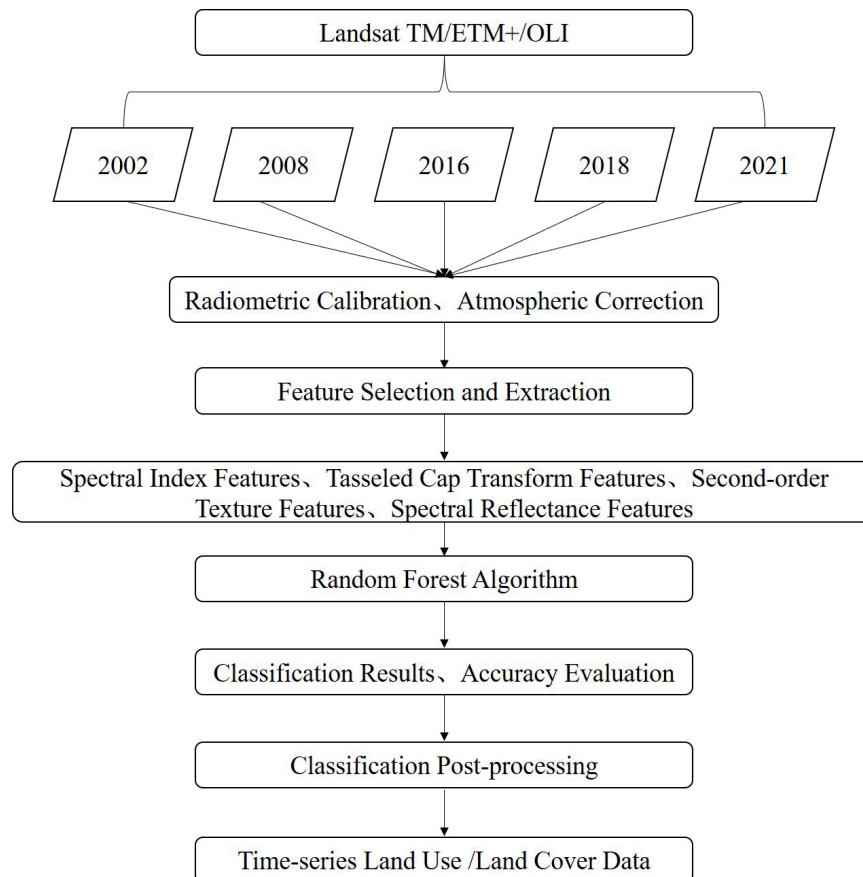


Fig. 2. Technical process for extracting land use information.

The tasseled cap transformation is a multispectral transformation method where the transformed axes point to directions associated with vegetation and soil [22, 23]: Brightness, Greenness, and Wetness [24]. In this study, the brightness, greenness, and wetness features obtained through tasseled cap transformation are utilized to enhance the separability between spectral features of similar land covers, thereby aiding in the identification of different types of vegetation.

Texture features play a crucial role in improving the accuracy of feature extraction [25, 26]. In this study, six minimally correlated texture features based on the Gray-level co-occurrence matrix (GLCM) are utilized: mean (MEA), standard deviation (STD), entropy (ENT), angular second-order moments (ASM), dissimilarity (DIS), and homogeneity (HOM) [27, 28], as shown below:

$$MEA = \sum_{i=0}^{N-1} \sum_{j=0}^{N-1} i \times P(i, j) \quad (4)$$

$$STD = \sqrt{\sum_{i=0}^{N-1} \sum_{j=0}^{N-1} P(i, j) \times (i - MEA)^2} \quad (5)$$

$$ENT = \sum_{i=0}^{N-1} \sum_{j=0}^{N-1} -P(i, j) \times \ln(P(i, j)) \quad (6)$$

$$ASM = \sum_{i=0}^{N-1} \sum_{j=0}^{N-1} P(i, j)^2 \quad (7)$$

$$DIS = \sum_{i=0}^{N-1} \sum_{j=0}^{N-1} P(i, j) \times |i - j| \quad (8)$$

$$HOM = \sum_{i=0}^{N-1} \sum_{j=0}^{N-1} \frac{P(i, j)}{1 + (i - j)^2} \quad (9)$$

where N represents the number of gray levels, P denotes the normalized gray-level co-occurrence matrix of size $N \times N$, and $P(i, j)$ represents the standardized gray-level value in the i th row and j th column of the matrix. This study only conducted second-order texture feature extraction for the green band [26], using a window size of 5 pixels by 5 pixels [18].

Classification Programming

The classification system developed in this study comprehensively considers multiple factors: (1) understanding the historical development of land use, geographic conditions, vegetation types, and farming methods in the study area; (2) analyzing the actual interpretability of the images used; (3) referring to the

national standard "Classification of Land Use Status GB/T 21010-2007." The developed classification scheme is shown in Table 1.

Sample Selection

In this study, a stratified random sampling method was employed for sample selection, with the sampling units being small polygonal blocks. Each small polygonal block contains 2 to 9 pixels, and it is assumed that all pixels within each small polygonal block belong to the same land cover type.

Random Forest Algorithm

Due to its high accuracy and effectiveness in handling large datasets, the random forest algorithm has been widely applied in the field of remote sensing [13, 29]. The principles of the random forest classification [13, 30] are illustrated in Fig. 3.

When using the random forest method for classification, it is necessary to set the number of decision trees forming the random forest (ntree) and the number of predictor variables randomly selected for decision tree splitting (mtry). In this study, ntree was set to an empirical value of 500, and mtry was set to the square root of the total number of input features [31].

Accuracy Evaluation

After training the model to classify remote sensing images, the accuracy of the classification results is evaluated using evaluation metrics generated from the confusion matrix: Overall Accuracy (OA) and Kappa coefficient (Kappa) [32]. The calculation formulas are as follows:

$$OA = \frac{\sum_{i=1}^c G_{ii}}{N} \times 100\% \quad (10)$$

where c represents the number of categories (same below), G_{ii} represents the number of test samples of category i correctly categorized into category i ($i = 1, 2, \dots, c$) (same below), and N represents the total number of samples in the test set (same below).

$$Kappa = \frac{P_0 - P_e}{1 - P_e}$$

$$P_0 = OA / 100\% \quad (11)$$

$$P_e = \frac{1}{N^2} \sum_{i=1}^c \left[\left(\sum_{j=1}^c G_{ij} \right) \times \left(\sum_{j=1}^c G_{ji} \right) \right]$$

Table 1. Yellow River Delta classification scheme.

Major category codes	First class categorization	Second class categorization	Minor category codes	Type description
1	Cropland	Wheat field	1	Areas used for growing wheat.
		Dry farmland	2	Areas including cotton fields, garlic, barns, and other crops.
		Paddy field	3	Mainly rice and lotus root.
2	Forest land	Woodland	4	Mainly planted acacia forests, willows, poplars, etc.
		Tamarisk shrub	5	Vegetation communities with tamarisk shrubs as the dominant species.
3	Grassland	Reed meadow	6	Vegetation communities with reed meadows as dominant species.
		Suaeda meadow	7	Predominantly suaeda meadow.
4	Impervious surface	Built-up area	8	Includes roads, parking plants, town sites, industrial and mining sites, etc.
		Rural Resident	9	Includes rural residential land and low-grade rural roads, etc.
5	Water	Fresh Water	10	Mainly includes reservoirs, rivers, ponds, canals, and other water bodies.
		Breeding aquatics	11	Includes mainly waters adjacent to the sea that are used for mariculture.
		Saltern	12	Comprises mainly areas used for salt production.
6	Tidal flat	undivided	13	Unvegetated land adjacent to the sea is susceptible to marine erosion.
7	Unused land	undivided	14	Mainly undeveloped bare land, fallow land.

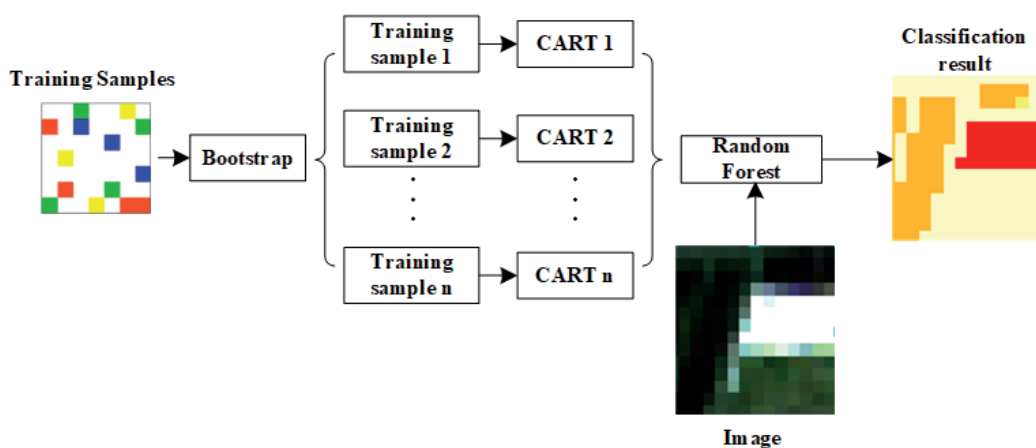


Fig. 3. Principles of the random forest classification algorithm.

where P_o represents the observed agreement rate, P_e represents the expected agreement rate, G_{ij} represents the number of test samples in category i that are categorized as category j , and G_{ji} represents the number of test samples in category j that are categorized as category i .

Results and Discussion

Classification Results and Accuracy Validation

The land use classification results of the Yellow River Delta wetland obtained from applying the model to the images of 2002, 2008, 2016, 2018, and 2021 are shown in Fig. 4. The accuracy evaluation metric calculation results are presented in Table 2.

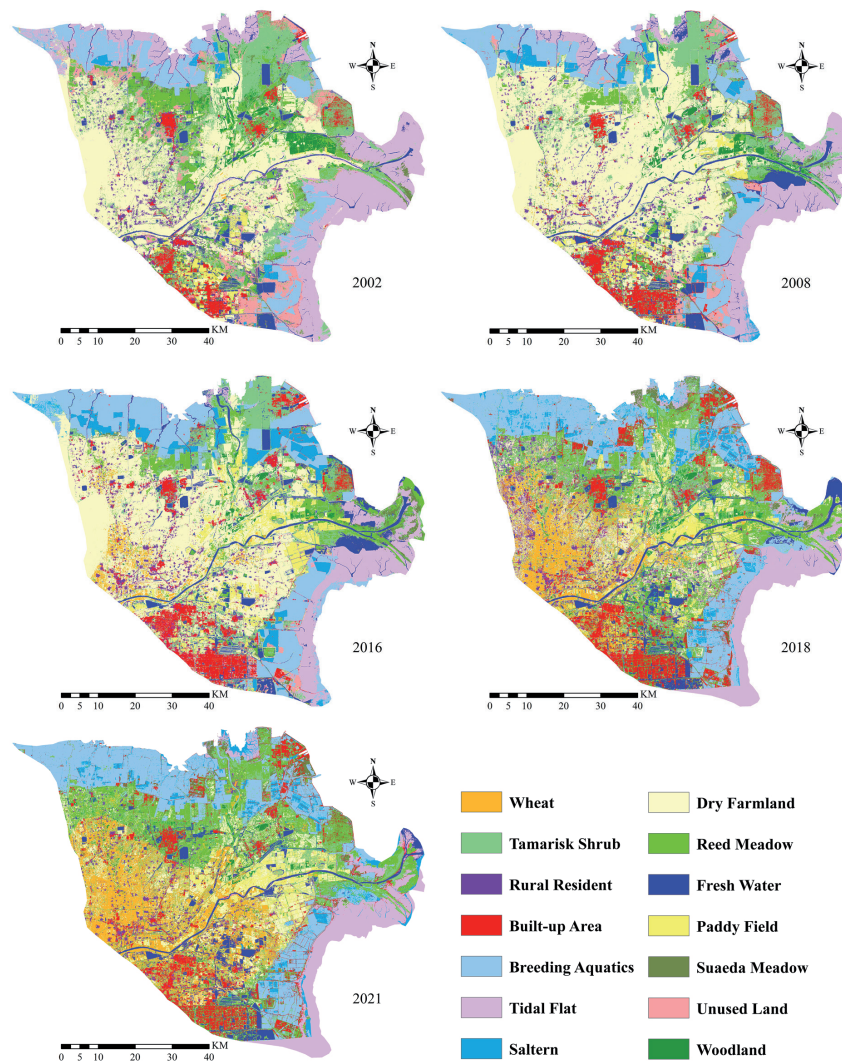


Fig. 4. Yellow River Delta land use classification results.

From the calculation results, it can be observed that the maximum OA was 91.4% in 2016, while the minimum was 89.0% in 2002, with an average of 90.5%. The maximum Kappa was 0.902 in 2016, while the minimum was 0.877 in 2002, with an average of 0.891. Hence, the land use classification results are quite satisfactory. This is mainly attributed to the multi-temporal data and selected features, which enhance the separability between different land cover types.

Table 2. Accuracy of land use mapping in the Yellow River Delta.

Year	OA	Kappa
2002	89.0%	0.877
2008	90.5%	0.888
2016	91.4%	0.902
2018	90.4%	0.890
2021	91.2%	0.900

Additionally, the random forest algorithm is capable of handling high-dimensional feature input data with excellent accuracy.

According to the classification results combined with actual field research, from 2002 to 2008, the built-up area was primarily concentrated in the central part of the Yellow River Delta, including Xicheng in Dongying District, Kenli Town in Kenli District, and the urban area of Hekou District. Subsequently, it was expanded to Dongcheng in Dongying District, Shikou Town, the urban area of Guangrao County, Dawang Town, Daizhuang Town, Shengtuo Town in Kenli County, and Chenzhuang Town and Yanwo Town in Lijin County. The expansion of Dongcheng stemmed from economic development driven by the Shengli Oilfield and the relocation of municipal government, while the expansion of townships was due to economic prosperity and increased infrastructure investment.

Wheat fields are predominantly cultivated in Guangrao County, where the soil is fertile and rivers provide water. Paddy fields are located in Xicheng,

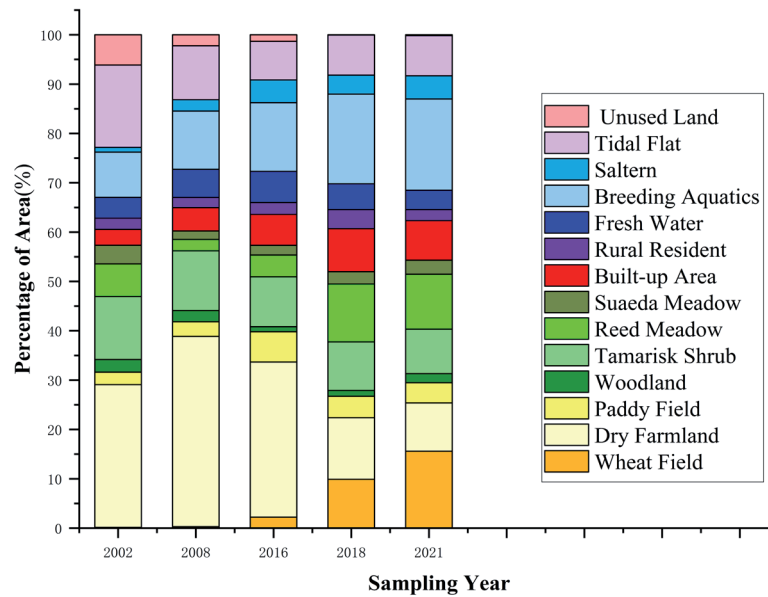


Fig. 5. Proportion of different land use types by year.

Dongying District, the urban area of Hekou District, and the high-standard farmland project area, benefiting from water sources from reservoirs and ponds. Tamarisk shrubs are found in the northeast, woodlands in the southwest of Gudao Town in Hekou District and the Yellow River Estuary National Nature Reserve, reed meadows in the northern part of the urban area of Hekou District and the reserve, and Suaeda meadows are near coastal mudflats. Unused land from 2016 to 2021 has been situated in the eastern part of Dongying District near the Guangnan and Guangbei reservoirs, the eastern part of Kenli District near inland areas, the northeastern part of Lijin County, and the western and southwestern parts of Hekou District. Tidal flats, breeding aquatics, and salterns are located in the northeast and east, adjacent to the Bohai Sea, and suitable for marine aquaculture. The fresh waters are found in the eastern part of Dongying District and Hekou District.

The article utilizes stacked histograms to illustrate the proportion of different land use types, as shown in Fig. 5. From 2002 to 2016, the proportion of cropland (wheat fields, dry farmland, and paddy fields) was the largest, indicating the significant importance of crop cultivation. However, the proportion of wheat fields and paddy field was relatively small, suggesting that grain crops did not dominate the planting structure. This is mainly due to the high degree of soil salinization and alkalization in the study area, as well as the scarcity of available water resources, which restrict the cultivation of wheat and rice [33].

Analysis of Land Use Changes

The Yellow River Delta wetland exhibits significant changes in land use types, as illustrated in Table 3. Studies indicate that from 2002 to 2021, there has been a substantial increase in cropland, impervious

surfaces, and waters, while woodland, grassland, tidal flats, and unused land have significantly decreased. The reduction in woodland is primarily attributed to its conversion to cropland, whereas unused land has mainly transformed into water, impervious surfaces, and cropland. Research suggests that the changes in land use types are influenced by multiple factors: location, hydrology, and soil conditions determine the overall pattern and trends of land use; population growth leads to the conversion of large areas of woodland and unused land into cropland; economic development results in the conversion of cropland around cities into built-up areas and the transformation of tidal flats and coastal saline-alkali land into breeding areas and salterns.

Analysis of Landscape Pattern Changes

Landscape patterns significantly impact the structure and function of ecosystems within a region [34, 35]. In this study, six landscape pattern indices were utilized, including the number of patches (NP) [34], patch density (PD), mean patch area (AREA_MN), landscape shape index (LSI), patch cohesion index (COHESION) [36], and aggregation index (AI) [35]. The calculation results are presented in Table 4.

From the calculation results, it can be observed that NP and PD in the Yellow River Delta decreased from 2002 to 2008, followed by a continuous increase from 2008 to 2021. Meanwhile, AREA_MN increased before 2008 and then steadily declined thereafter. These indices indicate that landscape fragmentation in the study area decreased before 2008 but has since been increasing. LSI exhibited a decrease followed by an increase around 2008, indicating that the shape of patches in the study area became simpler before becoming more complex. COHESION showed slight growth from 2002 to 2008, followed by a gradual decrease, with a slight

Table 3. Markov Transfer Matrix for the area of each land use type in the Yellow River Delta.

2021 \ 2002	Cropland	Woodland	Tamarisk shrub	Reed meadow	Suaeda meadow	Towns Land	Rural Resident	Fresh Water	Breeding aquatics	Saltern	Tidal flat	Unused land
Cropland	1666260	81015	291045	215625	21660	117150	53850	74100	58245	9615	5700	2760
Woodland	75945	29895	49440	28500	1470	5505	1845	4740	9600	3705	240	225
Tamarisk shrub	200085	9060	158130	227460	49815	111585	15765	25320	190440	44475	17235	2190
Reed meadow	176475	14205	77820	122325	10050	29550	5490	37125	53760	10215	3285	885
Suaeda meadow	71835	5385	41430	62625	6840	31395	2370	23820	41775	9900	13125	765
Towns Land	27975	1680	12255	35700	19305	139530	13635	5625	5505	1590	1485	270
Rural Resident	48045	1290	14220	9075	3390	24390	80955	3435	975	270	315	120
Fresh Water	33075	855	11565	29580	9630	20880	1830	138285	53205	19725	23985	3150
Breeding aquatics	11415	315	4515	14445	24795	40230	1080	9345	552675	77820	17010	315
Saltern	2100	45	810	2565	2610	4530	165	2895	50625	12465	975	45
Tidal flat	17370	1680	37260	87105	56970	59475	930	43905	389415	99465	572880	4590
Unused land	90480	6780	43110	78855	27570	74415	6690	32115	114090	18015	11355	570

Unit: acre

Table 4. Landscape pattern index of the Yellow River Delta from 2002 to 2021.

Year	Index					
	NP/each	PD/(each/km ²)	AREA_MN/km ²	LSI	COHESION/%	AI/%
2002	205096	37.436	2.671	202.823	99.276	83.742
2008	135818	24.791	4.034	151.997	99.561	87.864
2016	180132	32.879	3.041	187.807	99.441	84.963
2018	315883	57.658	1.734	308.726	98.015	75.152
2021	324906	59.305	1.686	327.033	98.855	73.665

increase from 2018 to 2021, suggesting that landscape connectivity increased initially, then decreased, and increased slightly again from 2018 to 2021. AI increased from 2002 to 2018 and then steadily decreased after 2018, indicating that different landscape patches were relatively dispersed from 2002 to 2008 and gradually aggregated thereafter.

In summary, the fragmentation, shape complexity, and aggregation of landscape patches in the Yellow River Delta wetland generally experienced a turning point around 2008, exhibiting a trend of decreasing followed by increasing. This is primarily attributed to the continuous expansion of cropland, impervious surfaces, and waters in the Yellow River Delta from 2002 to 2021, initially forming relatively large patches and maintaining a relatively continuous landscape with lower fragmentation. However, as activities continued, these patches were subdivided, leading to an increase in landscape fragmentation, shape complexity, and aggregation.

Conclusions

This study utilized Landsat-5/7/8 data and integrated surface reflectance features, spectral index features, tasseled cap transform features, and second-order texture features. Utilizing the random forest method, the images from 2002, 2008, 2016, 2018, and 2021 were classified into land cover types. The accuracy of the classification results was evaluated, and analyses of land use change and landscape pattern change were conducted. The main conclusions are as follows:

(1) The random forest algorithm achieved good results in land cover classification, with overall accuracy ranging from 89.0% to 91.4% and the Kappa coefficient ranging from 0.877 to 0.902.

(2) The built-up area in Dongying District and some townships expanded after 2008. Wheat fields are predominantly cultivated in Guangrao County, while paddy fields are found in Xicheng, Dongying District, the built-up area of Hekou District, and the high-standard farmland project area. Tamarisk shrubs are located in the northeast, woodlands in the southwest of Gudao Town in Hekou District and at the Yellow River Estuary National Nature Reserve, reed meadows in

the northern part of the built-up area of Hekou District and the reserve, and suaeda meadows near coastal tidal flats. Unused land from 2016 to 2021 was distributed in the eastern part of Dongying District near Guangnan and Guangbei reservoirs, in the eastern part of Kenli District near the inland, in the northeastern part of Lijin County, and in the western and southwestern parts of Hekou District. Tidal flats, breeding areas, and salterns are mainly located in the north and east. Croplands dominated the area from 2002 to 2016, but the proportion of food cropland was relatively small.

(3) The land use change in the Yellow River Delta wetland was drastic from 2002 to 2021, with increases in cropland, impervious surfaces, and waters and decreases in woodlands, grasslands, tidal flats, and unused land. Reduced woodlands have mainly been converted to cropland, while unused land has been converted to water, impervious surfaces, and cropland.

(4) Landscape pattern indices generally experienced a turning point around 2008. NP, PD, and COHESION first increased and then decreased, while AI, AREA_MN, and LSI first decreased and then increased. Thus, landscape fragmentation, shape complexity, and aggregation decreased from 2002 to 2008 and increased from 2008 to 2021.

Conducting mapping and landscape pattern evolution analysis in the Yellow River Delta wetland is of great significance for promoting regional sustainable development. This study will provide scientific support for regional development and help establish a more harmonious development model.

Acknowledgments

The authors thank USGS for providing the Landsat-8 OLI Data. This research was supported by Jinan City and University Integration Development Project (JNSX2023065).

Conflict of Interest

The authors declare no conflict of interest.

References

1. PAN Y.Y., JIANG B., LI M.Z., LIU X.Y. Spatial and Temporal Differences and Influencing Factors of Urban Land Use Efficiency in Three Provinces of Northeast China Based on Super-SBM Model. *Research of Soil and Water Conservation*, **31** (1), 408, **2024**.
2. AN B. On the Characteristics of Land-Use Evolution in Hanjiang River Ecological Economic Belt from 1985 to 2020. *Journal of Ankang University*, **35** (06), 16, **2023**.
3. ERIC A., THOMAS G.A., PHILIP A.A., ERIC A., ROBERT C.A., ERIK J., NEUMANN A. M., EMMANUEL B. Implications of changes in land use on soil and biomass carbon sequestration: a case study from the Owabi reservoir catchment in Ghana. *Carbon Management*, **14** (1), 1, **2023**.
4. BAH A., ZHANG H., LUO Z., HU J., ZHANG Z., XIE Y.L., YANG TING., CHEN G., BAH A. A study of land use changes and its impacts on flood inundation in the Konkoure River Basin, Republic of Guinea. *Environmental monitoring and assessment*, **196** (2), 212, **2024**.
5. CHENG Y., GUAN Y.H., WU X.Q. The spatial and temporal evolution of landscape pattern and landscape ecological security assessment in Karst Fault Basin based on land use change. *Acta Ecologica Sinica*, **43** (22), 9471, **2023**.
6. ZHAO F. Dynamic Monitoring of Land Use Change in the Yellow River Delta Based on Landsat. *Geomatics & Spatial Information Technology*, **45** (05), 124, **2022**.
7. LI J. On the Application of Hierarchical Extraction Method in the Yellow River Delta Wetland Information Extraction. *Geomatics & Spatial Information Technology*, **37** (11), 146, **2014**.
8. JIAO Y.B., TIAN X.Y., HU B.Q. Dynamic change and remote sensing information extraction of saline land in the yellow river delta – A case study in Shandong Kenli County. *Popular Science & Technology*, **18** (12), 31, **2016**.
9. XIAO Y., ZHAO G.X. Remote Sensing Monitoring and Driving Force Analysis of Land Use Changes in the Typical Area of the Yellow River Delta. *Geomatics & Spatial Information Technology*, **39** (09), 43, **2016**.
10. WANG L.L., FAN X.M. Analysis of the degradation evolution and driving factors of cultivated land in the Yellow River Delta based on the BFAST algorithm and multi-source data. *Journal of Geo-information Science*, **25** (11), 2218, **2023**.
11. CHANG C.Y., ZHAO G.X., WANG L., ZHU X.C., GAO Z. Land use classification based on RS object-oriented method in coastal spectral confusion region. *Transactions of the Chinese Society of Agricultural Engineering*, **28** (5), 226, **2012**.
12. FANY G., ZHANG L., SUN Y.F., WU T.T., ZHU H. The Research of Land Use Classification Monitoring of Yellow River Delta Region Using RS. *Remote Sensing Technology and Application*, **25** (01), 45, **2010**.
13. RODRIGUEZ-GALIANO V.F., GHIMIRE B., ROGAN J., CHICA-OLMO M., RIGOL-SANCHEZ J.P. An assessment of the effectiveness of a random forest classifier for land-cover classification. *ISPRS Journal of Photogrammetry and Remote Sensing*, **67**, 93, **2011**.
14. LIU C.T., MA Y., LIU X.Q. Integration of Multi-Source Remote Sensing Data for Spatial-Temporal Change Monitoring of Ecological Environment in the Yellow River Delta. *Polish Journal of Environmental Studies*, **31** (5), 4757, **2022**.
15. LIU J.T., LI Y.X., ZHANG Y., LIU X.Q. Large-Scale Impervious Surface Area Mapping and Pattern Evolution of the Yellow River Delta Using Sentinel-1/2 on the GEE. *Remote Sensing*, **15** (1), 18, **2023**.
16. DONG H.Z., CHI B.J., DAI J.L., ZHANG Y.J., CUI Z.P., ZHANG D.M. Strategies and Techniques for Eco-Efficient Crop Production in Saline-Alkali Land of the Yellow River Delta. *Shandong Agricultural Sciences*, **55** (3), 38, **2023**.
17. LU Q., XING S.H., LIU C., WANG S.C., CHEN M.Y., YUAN X. Spatiotemporal Variation of the Vegetation Coverage and Its Response to Land Use/Cover Changes in the Yellow River Delta in Recent 20 years. *Research of Soil and Water Conservation*, **30** (6), 366, **2023**.
18. SFENG Q.L., GONG J.H., LIU J.T., YI L. Monitoring Cropland Dynamics of the Yellow River Delta based on Multi-Temporal Landsat Imagery over 1986 to 2015. *Sustainability*, **7** (11), 14834, **2015**.
19. YE Z.X., ZHANG H.B., YANG Z.F., ZHANG Y.R., LI T.F., ZHAO X.W., XUE C.W. Spatial differentiation effects and risk detection of meteorological elements to vegetation cover on the Loess Plateau of northern Shaanxi. *Acta Ecologica Sinica*, **44** (06), 1, **2024**.
20. ZHAO Y.H., JIANG P.H., LI J.H., HAO Y.J. Extraction of forest burned area using SAVI based on Sentinel-2. *Journal of North China Institute of Science and Technology*, **18** (6), 27, **2021**.
21. XU H.Q. Modification of normalised difference water index (NDWI) to enhance open water features in remotely sensed imagery. *International Journal of Remote Sensing*, **27** (14), 3025, **2006**.
22. SHI T.T., XU H.Q., WANG S. Derivation of tasseled cap transformation coefficients for ZY-3 MUX sensor data. *Journal of Remote Sensing*, **23** (3), 514, **2019**.
23. ZHANG H.J., YANG L.J., SHI T.T., WANG S. Derivation of tasseled cap transformation coefficients for GF-6 WFV sensor data. *Remote Sensing for Natural Resources*, **1**, **2023**.
24. FU J.Q., CHEN C., GUO B.Y. A method of extracting shoreline information from remote sensing image based on Tasseled Cap transformation. *Science of Surveying and Mapping*, **44** (05), 177, **2019**.
25. LIU C.T., FENG Q.L., JIN D.J., SHI T.G., LIU J.T., ZHU M.S. Application of random forest and Sentinel-1/2 in the information extraction of impervious layers in Dongying City. *Remote Sensing for Natural Resources*, **33** (3), 253, **2021**.
26. FENG Q.L., LIU J.T., GONG J.H. UAV Remote Sensing for Urban Vegetation Mapping Using Random Forest and Texture Analysis. *Remote Sensing*, **7** (1), 1074, **2015**.
27. HARALICK R.M., SHANMUGAM K., DINSTEN I. Textural features for image classification. *IEEE Transaction on Systems, Man, and Cybernetics*. **SMC-3** (6), 610, **1973**.
28. HOU F., HU Z.L. Remote Sensing Information Extraction of Typical Surface Objects in a Coal Mining Area Based on Multiple-scale Segmentation. *Bulletin of Surveying and Mapping*, (01), 22, **2012**.
29. SHEYKHOUSA M., MAHDIANPARI M., GHANBARI H., MOHAMMADIMANESH F., GHAMISI P., HOMAYOUNI S. Support Vector Machine Versus Random Forest for Remote Sensing Image Classification: A Meta-Analysis and Systematic Review. *Ieee Journal of Selected Topics in Applied Earth Observations and Remote Sensing*, **13**, 6308, **2020**.

30. DONG H.Y., WANG Y.D., LI L.H. A Review of Random Forest Optimization Algorithms. *China Computer & Communication*, **33** (17), 34, **2021**.
31. BELGIU M., DRĂGUȚ L. Random forest in remote sensing: A review of applications and future directions. *Isprs Journal of Photogrammetry and Remote Sensing*, **114**, 24, **2016**.
32. LI Y., LI C.L., WANG X., FAN P.F., LI Y.K., ZHAI C.Y. Identification of Cucumber Disease and Insect Pest Based on Hyperspectral Imaging. *Spectroscopy and Spectral Analysis*, **44** (02), 301, **2024**.
33. XU J., LIU J.Z., ZHANG T.J., MA X.D., FU L., ZHANG Y.R., LI M., MA Y.Q., CHEN Y.J. Soil salinization characteristics under the crown of *Tamarix chinensis* in the wetland of the Yellow River Estuary. *Acta Ecologica Sinica*, **42** (17), 7118, **2022**.
34. LEI Y., ZHANG X.B., LUO J., LI Y.X., WANG Z.Y., YAO L.T., LI X.H. Spatio-temporal evolution of urban landscape pattern in arid areas based on different zones: A case study of Zhangye City. *Acta Ecologica Sinica*, **43** (5), 2034, **2023**.
35. NING Q., OUYANG H.Y., TANG F.H., ZENG Z.W. Temporal and Spatial Evolution of Landscape Pattern in Dongting Lake Area under the Influence of Land Use Change. *Economic Geography*, **40** (09), 196, **2020**.
36. HAN Y.H., SUN W.B., FU Y., YANG Y. Landscape pattern of built-up land in a typical mining city, Datong, Shanxi, China from 1986 to 2018. *Chinese Journal of Applied Ecology*, **32** (05), 1614, **2021**.